# Micrometer Sensing With Microwaves: Precise Radar Systems for Innovative Measurement Applications

**FABIAN MICHLER** [1] **(Student Member, IEEE), BENEDICT SCHEINER** [1] **(Student Member, IEEE),**
**TORSTEN REISSLAND** [1] **(Student Member, IEEE), ROBERT WEIGEL** [1] **(Fellow, IEEE),**
**AND ALEXANDER KOELPIN** [2] **(Senior Member, IEEE)**

*(Invited Paper)*

[1]Institute for Electronics Engineering, Friedrich-Alexander University Erlangen-Nuremberg, 91058 Erlangen, Germany
[2]Institute of High-Frequency Technology, Hamburg University of Technology, 21073 Hamburg, Germany

CORRESPONDING AUTHOR: Fabian Michler (e-mail: fabian.michler@fau.de).

**ABSTRACT** Radar sensors have been widely used to estimate speed and displacement of remote targets. A novel market for contactless radar sensing is emerging in the field of automatization and process analysis, where non destructive testing and evaluation methods are desired. Here, modern radar systems offer various advantages over conventional sensors since they enable the contactless, continuous, and cost-efficient measurement of static or dynamic ranges. These can further be used for vibration and vital sign characterization. Advances in microwave technology, an increasing integration density, and the development of novel algorithms keep boosting the performance of the systems. After introducing the most common operation principles, such as unmodulated and frequency-modulated continuous-wave radar, different design aspects and building blocks of cutting-edge systems are explained in detail. In the second part, selected applications are described in detail. These include the sheet thickness monitoring of metallic foils, and the measurement of the ground speed of vehicles with the latest approaches. Exemplary low-power radar systems are presented to show the limits in terms of power consumption while still offering a high measurement precision. In addition, the topics of mechanical vibration sensing and vital sign sensing are addressed by introducing tailored systems.

**INDEX TERMS** Radar theory, radar remote sensing, Doppler radar, radar applications.

## I. INTRODUCTION

During the past decades, radio detection and ranging (radar) has been a quickly growing field of research within the microwave engineering community. An impressive indicator supporting this statement is the number of new scientific publications listed in the electronic database IEEE Xplore under the keyword *radar* as shown in Fig. 1. The count of new contributions per year has shown an almost exponential growth and exceeded 10,000 new publications in the year 2019.

This technological success story results from the physical properties of microwaves, which can propagate the free space and non-metallic materials. By controlling different properties

of a transmitted electromagnetic wave, the reflection caused by a target can be received and evaluated. Depending on the modulation scheme, parameters like target position or speed can be measured. Moreover, valuable information on dielectric and conductive properties of the target is contained in the reflected signal and can hence be evaluated. Due to the non-ionizing character of microwaves, they do not cause any harm to humans if low transmit powers are used as it is demanded by the regulations of the responsible authorities. The remote sensing of the physical properties of an object is a highly desired ability in multiple fields of application. Starting with the detection of ships in the fog around the year 1900 as first commercial application, the concept was
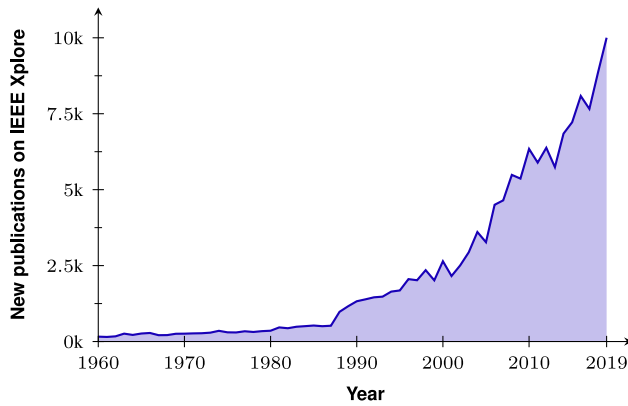
**FIGURE 1.** New IEEE Xplore search results per year for the search term "radar".

extended to the monitoring of airplanes and later used for radio astronomy [1].

Today, radar-based remote sensing systems are used in many fields of application: A big sector are industrial applications, where the positions and quantities of tools and goods need to be tracked continuously to increase efficiency. Examples are the measurement of levels of fluids and solids in storage tanks [2]–[4], where a radar sensor is preferred over conventional systems to avoid direct contact to the sample. Especially if oil or gas at a high pressure is used, for example to displace pistons or hydraulic cylinders, radar systems are an attractive alternative [5]–[7].

An early fault detection can help to decrease the reject rate, for instance by monitoring the thickness of foils and sheets during fabrication [8] or the vibrations of machines [9], [10]. In an industrial measurement setting, dust and mist can be contained in the air between sensor and target, or temperatures of the target might be extreme. While most conventional contactless sensors work in the optical domain and hence suffer from diffraction and absorption in these harsh environments, microwaves can penetrate dielectric media in many cases.

This advantage over optical sensors is a key feature of automotive radars, which are used to produce images of the cars' surroundings - even at night and during strong rain. Automotive sensors and radar imaging are addressed by the article by Christian Waldschmidt *et al.* in this issue. One of the most recent use cases of radar systems is the detection of vital parameters. Based on a continuous distance measurement between system and patient, vital parameters such as respiration or heart rate can be detected. This topic is covered in detail in this issue by the article by Changzhi Li *et al.*

In addition to the growing list of applications, the increasing research activities on radar technology find their reason in the growing complexity of the systems. While the first prototypes only provided a presence detection, modern systems offer a precision in the micrometer range, even at a very compact size and a low power consumption. The design process of these highly developed systems covers a broad range of topics from tailored integrated circuits and radio

front-ends to the development of dedicated algorithms for signal processing. Thus, a joint work of multiple disciplines, from semiconductor research to packaging and system-level engineering to machine learning is required.

This article reviews the most common operational principles and system concepts of modern radars and provides an insight into the critical aspects of the system design. In the second part, application examples are presented and described in detail. This focuses on the industrial domain with sheet thickness and vehicle speed measurements. Moreover, examples on both low-power and high-precision systems are given and vibration analysis is discussed through the examples of mechanical vibration analysis and vital sign sensing.

## II. RADAR FUNDAMENTALS

When designing a radar system for a specific application, the first step is always the careful choice of system architecture and modulation technique. As shown in Table 1, different modulation schemes have an impact on features and requirements of the sensing system. In the following sections, the most common modulation techniques of radars will be presented.

### A. UNMODULATED CONTINUOUS-WAVE RADAR (CW)

The simplest transmit waveform for a radar system is an unmodulated sinusoidal signal of constant frequency, called continuous-wave (CW) radar. The introduced time delay from system to target and back causes a phase shift $\Delta\varphi$ between sent and received waveforms, which can be translated into a displacement $\Delta R$ using the known signal wavelength $\lambda$:

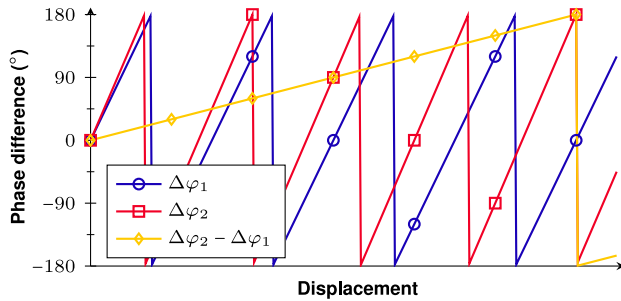$$\Delta R = \frac{\Delta\varphi}{2\pi}\frac{\lambda}{2} \tag{1}$$

Due to the periodicity of the sinusoidal signal, the ambiguous range is $\lambda/2$, which is fairly small for micro- and millimeter-waves. Hence absolute positions cannot be determined, but a relative displacement starting from a reference position can be analyzed. If the measured phase is sampled fast enough, a phase unwrapping can be done and relative displacements which exceed the unambiguous range can be recorded. The unambiguous range can also be extended, if the distance-dependent power of the backscattered signal is taken into account (see section III-III-A). The clear advantage of using an unmodulated carrier is the theoretically infinitely narrow (RF) bandwidth of the carrier, which can thus be generated with a very low phase noise. Together with a narrowband baseband signal processing chain, a low standard deviation of the displacement measurement in the single-digit micrometer range and below can be achieved. Another advantage of this technique are the low costs of the components and the high power efficiency.

### B. MULTI-TONE RADAR

To increase the unambiguous range of the CW radar, several discrete transmit frequencies can be used alternating in time [11]–[13]. If, for instance, two frequencies $f_1$ and $f_2$ are

**TABLE 1.** Comparison of Different Modulation Schemes Regarding Their Properties and Advantages

| Modulation | Speed measurement | Absolute distance | Target separation | Unambiguous range | Hardware complexity | Required bandwidth |
|---|---|---|---|---|---|---|
| CW | yes | no | no | very small | low | very low |
| Multi-tone | yes | yes | no | small | low | low |
| FMCW | yes | yes | yes | large | medium | medium-high |
| UWB | yes | yes | yes | large | medium | high |



**FIGURE 2.** Extended unambiguous range by using a dual-tone transmit signal.



**FIGURE 3.** Linear frequency chirp as exemplary frequency-modulated continuous-wave (FMCW) transmit waveform and corresponding receive signal for a static target.

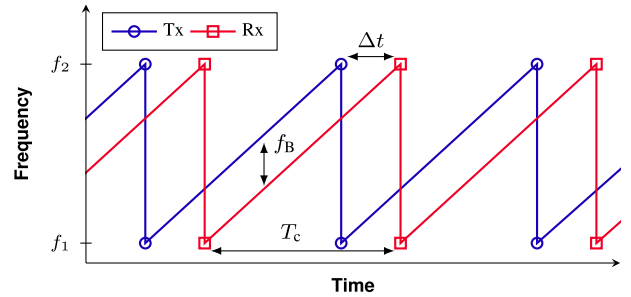used, the unambiguous range can be extended to

$$R_{\max} = \frac{c}{2(f_2 - f_1)} \qquad (2)$$

as shown in Fig. 2. Here, $c$ denotes the propagation speed of the electromagnetic wave in the medium, for example $3 \times 10^8 \mathrm{ms}^{-1}$ in vacuum. The use of the second tone hence leads to an improvement of a factor of $f_1/(f_2 - f_1)$ in contrast to the single-frequency case ($f_1$). It is evident that a closer spacing of both frequencies increases the unambiguous range, but the system becomes more sensitive to noise and has to provide an even higher signal-to-noise ratio (SNR). If the number of used frequencies is increased, degrees of freedom can be used to compensate for system nonlinearities. Occupying only a low bandwidth but still offering a large unambiguous range, this modulation technique is a compromise between CW and (FMCW) radar.

## C. FREQUENCY-MODULATED CONTINUOUS-WAVE RADAR (FMCW)

Especially in industrial and automotive applications, FMCW radar is a commonly used modulation scheme. It can be seen as an extension of the multi-tone modulation with a continuous change in frequency, which is called chirp. An exemplary signal with a linear chirp of duration $T_c$ is shown in Fig. 3. For a static target, the receive (Rx) signal equals the transmit (Tx) signal but with a time delay of $\Delta t$. The receiver determines the frequency difference $f_B$ of both signals, for example using a mixer in the analog domain, and a fast Fourier transform (FFT) after digitization. The absolute range of the target $R$ can then be calculated by

$$R = c\frac{\Delta t}{2} = \frac{c f_B T_c}{2B}, \qquad (3)$$

where $B = f_2 - f_1$ denotes the used bandwidth. The resolution of the distance measurement is given by $c/(2B)$, i.e. a larger bandwidth leads to smaller range bins. While modern monolithic microwave integrated circuit (MMIC) technology can achieve transmit bandwidths of up to 60 GHz [14], [15] and hence reach a resolution in the single-digit millimeter range, the use of these systems in unshielded environments is strongly limited by legal regulations. By using fast chirps, the phase information of subsequent received ramps can be processes to obtain the Doppler information of moving targets. Using this so-called micro-Doppler, an accuracy of few micrometers is achievable [16], [17]. A big advantage of FMCW over unmodulated carriers is the ability to separate multiple targets at different ranges, which is an inherent feature of the spectral analysis of the intermediate frequency (IF) signal.

## D. ULTRA-WIDEBAND RADAR (UWB)

In contrast to the mentioned CW radar architectures, ultra-wideband (UWB) radars use short pulses as transmit signals. After calibration of cables and antenna, the time delay between sent and received equals the time-of-flight and hence the distance, a Doppler processing reveals the target speed. Due to the short temporal duration of the pulses in the picosecond range, the occupied spectrum is large, leading to a low power density as required by the regulations [18]. Special waveforms with optimized correlation functions, such as pseudo-random noise or maximum-length sequences are often used to increase SNR and range [19]. The clear advantage of the large radio frequency (RF) bandwidth is an improved robustness, especially in multipath scenarios and frequency-selective channels, like through-the wall imaging and localization of humans buried under debris [20].

## III. SYSTEM DESIGN

Having understood the most common modulation schemes for continuous-wave radars, the major system design aspects, including the choice of operation frequency and the entire signal chain, will be described in this section.

### A. CHOICE OF OPERATION FREQUENCY

When designing a radar system, one of the first decisions to be made is the operation frequency. Although there are exceptions, most of the commercially available radars are operated in the microwave spectrum, which is a common name for the spectral range from 300 MHz to 300 GHz. The sub-band starting from 30 GHz (wavelength 10 mm) is also called millimeter wave band [21]. If for instance a phase resolution of $1°$ is assumed for the receiver, displacements of 1.4 mm down to 1.4 $\mu$m can be detected and thus justify the names given to the frequency bands. In various publications it has been shown that distance measurements on a micrometer scale are achievable with microwave radars [22]. It is clear that increasing the operation frequency improves the distance resolution. However, further side-effects, such as a decreased detection range, need to be taken into account as well.

To calculate the received power $P_{rx}$ of a radar system, which transmits a power $P_{tx}$ and illuminates a target of cross-section $\sigma$ at distance $R$, the well-known radar equation can be used. It is given by

$$P_{rx} = \frac{P_{tx}D_{tx}}{4\pi R^2}\sigma\frac{1}{4\pi R^2}\frac{\lambda^2 D_{rx}}{4\pi}, \tag{4}$$

assuming lossless antennas with directivities of $D_{tx}$ and $D_{rx}$, respectively [23]. It is obvious, that a high operation frequency leads to short wavelengths $\lambda$ and hence decreases $P_{rx}$, which lowers the SNR at the receiver at a given noise floor. The directivity $D$ of antennas, however, scales with

$$D = \frac{4\pi A_e}{\lambda^2}, \tag{5}$$

where $A_e$ stands for the effective aperture [23]. Thus, a high operation frequency requires smaller antennas to achieve a desired directivity, which is also linked to the area illuminated by the system. The frequency-dependence also applies to any narrowband structures, such as couplers, filters, or matching networks and hence affects the integration density of systems. In addition, the size of RF circuits is related to the use of propagating structures whose dimensions are wavelength-dependent. Another point to consider are dielectric losses of the used materials and frequency-dependent absorption losses of the propagation medium, which cause an additional signal attenuation. The choice of operation frequency is always a trade-off between the aforementioned parameters and highly depends on the specific application.

A further point worth mentioning are the legal constraints. Since spectrum is a limited and shared resource, all users must confer to common regulations. The International Telecommunication Union (ITU) defines the so-called Radio Regulations, which assign the spectrum to different services. For

**TABLE 2.** Microwave and Millimeter-Wave ISM Bands as Defined by the ITU [24]

| Center frequency (GHz) | Bandwidth (MHz) |
|:---:|:---:|
| 2.45 | ±50 |
| 5.8 | ±75 |
| 24.125 | ±125 |
| 61.25 | ±250 |
| 122.5 | ±500 |
| 245 | ±1,000 |

general purpose microwave-systems, the industrial, scientific and medical (ISM) bands in the microwave and millimeter-wave ranges, which are listed in Table 2 allow a license-free operation. However, the radiated power should be "minimal" and not interfere with other services, like navigation [24]. Individual regulations on the national level refine these limits, especially regarding transmit power.

### B. SIGNAL GENERATION

To generate the transmit signal of microwave- and millimeter-wave radars, voltage controlled oscillators (VCOs) are the most common building blocks. They convert an applied DC power into a sinusoidal output signal with a defined frequency, which can be tuned by additional control voltages. If even higher operation frequencies are desired, an optional frequency multiplier can be added. Since VCOs are semiconductor devices, their resonance frequency is temperature-dependent. Moreover, process parameters and package also affect the output. For the most basic CW radars, the voltage controlled oscillator (VCO) can be used in a free-running mode, leading to low system complexity costs and power consumption [25]. However, this also means a varying transmit frequency, thus a poor phase noise and a large standard deviation of the range measurement. For unmodulated CW radars, this effect was described analytically by [26], [27]. Moreover, it was shown that a close target leads to a strong correlation of sent and received phase noise due to the short propagation time, causing a smaller root mean square (RMS) distance error. The effects of target range and baseband bandwidth on measurement precision are shown in Fig. 4 for the case of a free-running and a phase-locked loop (PLL)-controlled VCO at 24 GHz.

### C. RECEIVER ARCHITECTURES FOR CW RADARS

The task of the receiver is the downconversion of the incoming RF signal to the equivalent baseband voltages, which do not contain the carrier anymore. This is done by a mixing process in the analog domain, where a fraction of the Tx signal, called local oscillator (LO), and the Rx signal are multiplied through a nonlinear device. The product of two sinusoidal signals in time domain is the equivalent of a convolution in frequency domain, resulting in the sum and difference frequencies of both input signals. A low-pass filter (here denoted as LP{·}) then rejects the upconverted frequency components. The downconversion of the unmodulated CW radar signal can
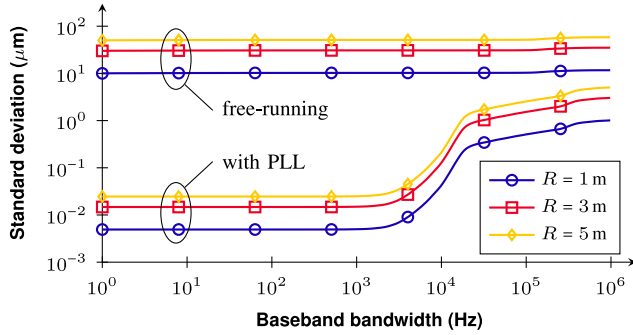
**FIGURE 4.** Standard deviation of a 24 GHz CW radar system in dependence of bandwidth and target range. The phase noise improvement by the PLL-controlled VCO clearly enhances the measurement precision compared to the free-running VCO [27].



**FIGURE 5.** Block diagram of a quadrature-mixer based downconversion for continuous-wave radars.

be interpreted in two different ways, which are both mathematically equal:

First, if a moving target is considered, a Doppler shift of $f_D$ will occur. The mixer then determines the frequency difference of sent and received signal, and the Doppler equation translates this into a speed, which can be integrated to obtain the target displacement.

$$\text{LP}\{\underbrace{\sin(2\pi f_{\text{tx}} t)}_{\text{LO signal}} \underbrace{\sin(2\pi (f_{\text{tx}} \pm f_D)t)}_{\text{Rx signal}}\} = \frac{1}{2}\cos(\pm 2\pi f_D t) \quad (6)$$

Because of the actual estimation of Doppler frequency, this is oftentimes called *Doppler Radar* in literature.

The second point of view first assumes a static target, resulting in equal Tx and Rx frequency. If the target starts to move linearly, the phase of the received signal changes linearly as well:

$$\text{LP}\{\underbrace{\sin(2\pi f_{\text{tx}} t)}_{\text{LO signal}} \underbrace{\sin(2\pi f_{\text{tx}} \pm \varphi)}_{\text{Rx signal}}\} = \frac{1}{2}\cos(\pm\varphi) \quad (7)$$

The phase result can then be translated to a displacement using (1). Because the phase difference of two RF signals is evaluated, this is often called an *Interferometer* in literature.

No matter which perspective is chosen, the information is always contained in a cosine function. However, due to its symmetry, its argument's sign and hence the direction of target movement cannot be determined. This might be tolerable for a simple presence or movement detection [28], but usually the direction matters. The solution to this problem is the quadrature downconversion, which uses a second multiplication with the LO phase delayed by $-90°$. As shown in Fig. 5, two baseband signals, the so-called inphase (I) and quadrature (Q) signals, are obtained and the receiver is hence commonly called an *IQ Demodulator*. The mixing process can be done for all above mentioned modulation schemes.

### 1) QUADRATURE MIXING

For the downconversion different architectures are possible. The quadrature mixer (Fig. 5) is an active nonlinear device with two input ports and an output port. In microwave and
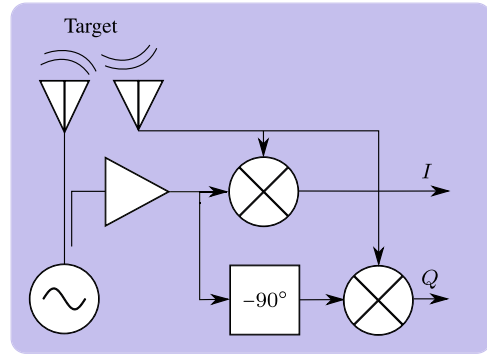
millimeter wave radars, the multiplication of LO and Rx signal is oftentimes done by a Gilbert cell and the delayed version of the LO signal is generated by a polyphase filter [29], [30]. Quadrature mixers can achieve large bandwidths and a high integration density [31]. This has made them cheap mass products. Their major disadvantage is the high LO power required to establish the operation point (typically 10-13 dBm), which makes them unsuitable for ultra-low power applications.

### 2) SIX-PORT RECEIVER

An alternative architecture for the quadrature receiver is the so-called six-port network. First published by Engen *et al.* under this name in the 1970s, this passive network was primarily used as low-cost alternative to network analyzers for microwave component and circuit analysis [32]. An important milestone in the history of the six-port was the development of a digital receiver for microwave and millimeter-wave communications at the Poly-Grames Research Centre of the École Polytechnique de Montréal, Canada [33], [34], followed by the development of six-port based modulators, making it a suitable communication front-end for high bandwidths and data rates [35]–[37]. This success story was also picked up by radar engineers, using the six-port for distance measurements [38].

The operation principle is as follows: The six-port network superimposes the two input signals Rx and LO by introducing phase shifts of multiples of 90° as shown in Fig. 6. Thus, four output signals are created, which are fed to power detectors, each consisting of a self-biased Schottky diode and a low-pass filter in the simplest case. Their output signals correspond to differential I and Q signals. The LO power may be as low as the Rx signal and the receiver does not require any bias, which makes it perfectly suitable for low-power and low-complexity applications [25].

The passive network can be fabricated in a very cost-efficient way on printed circuit board (PCB), for instance as substrate integrated waveguides [39], microstrip lines, or in coplanar technology [40]. Moreover, it can be scaled and adapted to almost any frequency of interest. Especially high
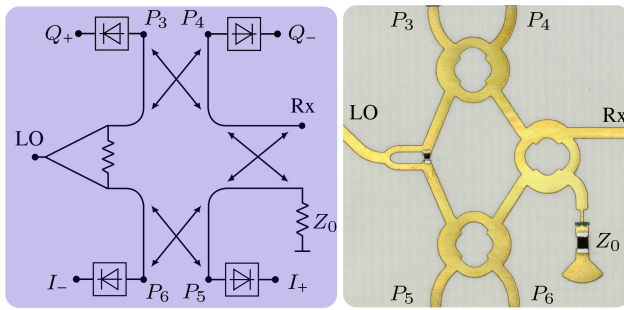
**FIGURE 6.** Block diagram of the six-port with detectors (left) and photograph of a microstrip layout (right) of the passive six-port network.
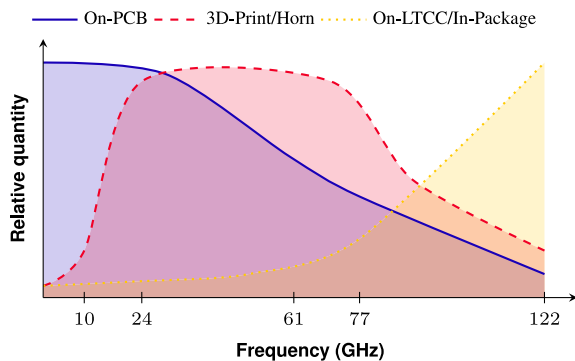


**FIGURE 7.** Relative quantity of used antenna technologies for compact radar systems.

frequencies are attractive due to short wavelengths and the resulting small structure sizes. Starting in 1992 with the first monolithic implementation of the six-port [41], hybrid [42] and fully integrated devices have been presented for both communications and radar purposes, and frequencies up to 120 GHz could be achieved [43].

## D. ANTENNA AND TRANSITION DESIGN

The antenna design itself depends on the specific radar application scenario. This means that the following considerations do not only include industrial but also vital sign and automotive radar scenarios where antennas have to be integrated into compact systems. If unmodulated CW or ISM-compatible FMCW systems are considered, a narrow-band antenna is oftentimes sufficient.

As already mentioned above the chosen operation frequency of the system is mainly determined by the given application. Of course this choice directly influences the antenna design since a higher frequency leads to a smaller wavelength and consequently to smaller antenna sizes [23]. An overview of the relative quantity of different antenna technologies in compact radar systems depending on the operation frequency is given in Fig. 7. The quantities rely on a qualitative literature research in IEEE Xplore, which was conducted by the authors. The technologies are clustered to on-PCB [28], [44], 3D-printed and horn antennas [45], [46] as well as on-LTCC, on-chip and in-package antennas [47], [48], respectively. Since

wavelength is comparably long at lower frequencies, mostly patch antennas on-PCB are used in this domain. However, at higher frequencies substrate losses increase, reducing the efficiency. Furthermore, substrate tolerances regarding height and permittivity have stronger effects on the antennas' behavior. Nevertheless, planar on-PCB antennas are commonly used in the automotive band around 77 GHz due to their compact size and cost effectiveness. Examples are published up to more than 120 GHz [49]. By taking a look at the class of 3D-printed and horn antennas, it is clear that at lower frequencies these antennas have to be very large and are thus very costly. In contrast to this, 3D-printing tolerances and roughness limit the upper frequency bound, which will be certainly extended during the ongoing development of 3D-printing. Conventional horn antennas are available up to very high frequencies but become expensive at the same time and require a low-loss, wideband transition to the PCB [50]. The third antenna technology worth mentioning is formed by on-LTCC, on-chip and in-package antenna types. The first is often used in automotive radars in 77 GHz range to further save space [51]. At even higher frequencies the main approach is to integrate antennas directly on chip or in package, which is possible due to the short wavelength and consequently small resonant structures. This way, there is no need to set high requirements on the interconnects to the PCB and its substrate since the complete RF part is contained within the RF package.

As already mentioned, the antenna has to be selected according to the specific application which means that in a scenario where multiple targets arise but no separation is possible since an unmodulated CW signal is used, it is necessary to focus the beam as much as possible and suppress side lobes in the antenna pattern. This, however, can only be done by a larger aperture, which increases the size of the overall system. At higher frequencies the antenna gain is usually improved by dielectric lenses that are placed on top of the integrated circuits (ICs) with integrated antennas [52], [53]. Consequently, this is always a trade-off between size and gain of the antenna, and a consideration of the measurement scenario.

## E. ANALOG SIGNAL CONDITIONING

After downconversion of the RF signals the baseband should be processed in analog first to reduce the demands on analogto- digital converters (ADCs) and digital processing units. Thus this analog signal conditioning is essential to increase SNR and consequently improve the overall performance of low-cost and compact systems.

In Fig. 8 a general block diagram of a baseband circuit is depicted. By considering a CW radar it is firstly important to determine if the signal can be AC coupled. This can be done if comparably fast target movements are expected. In this case a capacitor value with low impedance for these signal components is connected in series. Due to this, the DC offset is blocked. However, for low target speeds the capacitor value can become very high such that the signal has to be DC coupled. This means that the offset has to be compensated in a
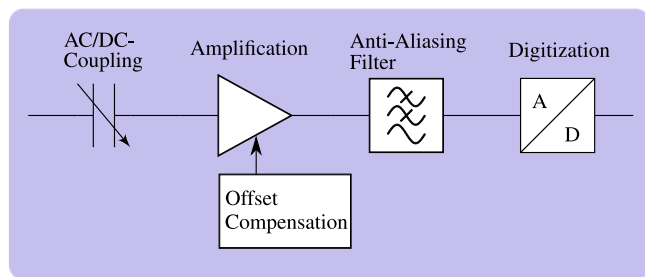
**FIGURE 8.** Block diagram of an exemplary baseband circuit.



**FIGURE 9.** Influence of offset shifts on the phase measurement of a CW-radar. Undesired DC offsets in the I/Q signals distort the linear relation between target distance and measured phase angle as seen from the origin of the axes.

subsequent stage [54]. Even though several offset compensation techniques have been presented, the signal should be AC coupled if possible to reduce complexity. This is one of the advantages of FMCW systems, where signals can generally be AC coupled due to the intermediate frequency. As shown in [55] it is further possible to perform the offset cancellation in the RF part.

In the next stage the signal is amplified to maximize the modulation of the ADCs which thus leads to a higher SNR. If DC coupling is applied, the amplifier can also be used to subtract a defined offset. Afterwards a low-pass filter follows the amplifier circuit to reduce the noise at high frequency [56]. This is necessary to fulfill the Nyquist criterion of

$$f_s > 2 \cdot f_{\max} \tag{8}$$

with sampling frequency $f_s$ and maximum signal frequency $f_{\max}$ in order to prevent aliasing. Depending on the maximum expected target speed $v$ the minimum bandwidth of the low-pass filter can be estimated by

$$B_{\min} = \left( \frac{1 + \frac{v}{c}}{1 - \frac{v}{c}} - 1 \right) \cdot f \approx \frac{2vf}{c} \tag{9}$$

where $c$ is defined as the known speed of light and $f$ the signal frequency.

By using fast ADCs filtering can also be done in the digital part [57]. However, depending on the scenario filters should be designed in different types and typologies that have to be selected. Of course a filter before the amplification stage is also possible and would further reduce the noise before the signal is amplified [58]. As proposed in [59] the AC coupling and anti-aliasing filter can be combined to a bandpass filter. Since radar transceivers usually have two or four baseband outputs to form either a single-ended or differential I/Q signal, respectively two or four single-ended or two differential ADCs are necessary to digitize the baseband signals. The sampling rate has to meet the Nyquist criterion as well and higher resolution improves the SNR. Particularly relevant is the information of the effective number of bits.

### F. SIGNAL PROCESSING
After digitization the data are processed in the digital domain. For evaluation purposes, the process can be done offline. However, for real-time applications the signal processing
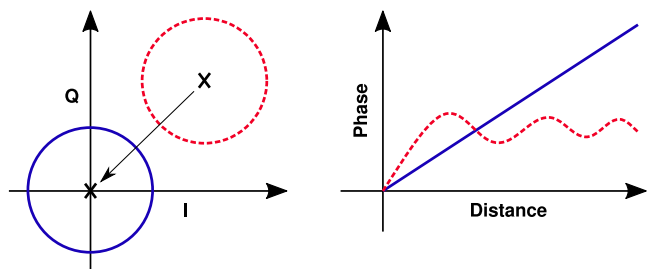
should be run in an embedded environment like a microcontroller. For Doppler radars, state-of-the-art microcontrollers are capable to perform this task since only a phase evaluation has to be performed. Often, integrated ADCs are sufficient which are available up to 16 bit [46] that leads to a low-cost integrated solution.

For a linear target movement and a resulting linearly changing phase angle $\varphi$ between sent and received signal, the in-phase signal is a cosine according to (7), and the quadrature signal a sine. The phase angle can thus be obtained by the arctangent of the quotient of both [40]:

$$\varphi = \arctan \left( \frac{Q}{I} \right) \tag{10}$$

If both orthogonal components are drawn versus each other as axes of a Cartesian coordinate system, a circle will result, where each point in time corresponds to a point on the circle. This is equivalent to the interpretation of I and Q as real and imaginary parts of a complex baseband signal, whose phase angle again equals $\varphi$.

Real radar systems, however, often suffer from phase and amplitude imbalances due to imperfect components and non-linearities mainly in the RF circuit. This leads to stretched and shifted circles in the I/Q-plane and consequently decrease the measurement accuracy [60]–[62]. Due to this, many correction algorithms have been presented to map the elliptically stretched circled to a unit circle [60]. This can be done in software [61], [62] or with the help of hardware components like phase shifters in the RF domain [63]. Each time the system is installed in a new scenario, this calibration has to be performed again. In Fig. 9 the influence of a shifted offset on the measured phase of an ideal circle in an I/Q diagram can be seen.

## IV. APPLICATION EXAMPLES
After having explained the concept of modern high-precision radars and described the important points in system design, selected application examples will be presented in this section.

### A. THICKNESS MONITORING
During the industrial production of sheets of different materials like steel or plastic, it is important to monitor the sheet

thickness to ensure high quality. For example in steel rolling mills the sheet thickness has to be continuously measured to compensate for arising deviations [64]. Especially in cases of hot or fragile materials a contactless way of measuring the sheet thickness is to preferred. The usage of radio frequency or millimeter wave based systems offers the advantage of a generally higher robustness in harsh environments compared to optical systems.

The approach described in [65] is based on a radio frequency interferometer working in the X-band. Its intended use is the measurement of a metal sheet's absolute thickness. In the presented setup two antennas are placed on both sides of the sheet. A signal is fed into the first antenna, reflected and received again. The received signal is guided through a directional coupler to the second antenna, reflected by the other side of the sheet and received again. By the use of a second directional coupler and a Wilkinson divider it is added to a reference signal. Thus, the signal travels the distance of all cables and passive structures plus the respective distances between both antennas and the metal sheet. The resulting signal is then detected and digitized. If the electrical distances of reference signal and the measurement signal differ by an odd multiple of $\lambda/2$, a destructive interference occurs and the resulting signal tends to be zero. The operation frequency is variable and therefore several zeros in the resulting signal can be observed within the interval of operation frequencies. Disregarding a certain ambiguity, these zeros allow to determine the distance traveled by the measurement signal and can therefore be used to measure the sheet's thickness. The authors expect a measurement accuracy of a few micrometers, though they lack a proof. Nevertheless, it is shown that the approach works in principle, but requires calibration techniques, both in the analog and digital domain to overcome system imperfections, differing signal amplitudes and unknown electrical distances.

In [8] an approach based on a similar idea is presented. The metal sheet of unknown thickness is placed between two antennas, but in this approach the antennas belong to two independently operating CW radar systems operating at 61 GHz. The system is intended to be used in monitoring changes in the sheets thickness during production. It is not able to deliver absolute thickness measurements but relative changes with high precision. This is caused by the fact that it solely relies on phase measurements at a single frequency. The changes in thickness are simply calculated by subtracting the phase measurements from both radars. It was tested with the setup shown in Fig. 10. For evaluating the system an aluminum sheet with several shaped steps of about $100\,\mu\mathrm{m}$ height was produced. The measurement results using this sheet are shown in Fig. 11. The system makes use of the aforementioned six-port receiver and achieves precisions of about $10\,\mu\mathrm{m}$ making it superior compared to other radar based approaches as shown in [8].

In [66] a method for determining the width of multiple layers of dielectrics on a conducting substrate is presented. Such a technique is e.g. applied in quality assessments in aircraft manufacturing. The setup consists of a waveguide probe which is placed on the coating to be measured. The
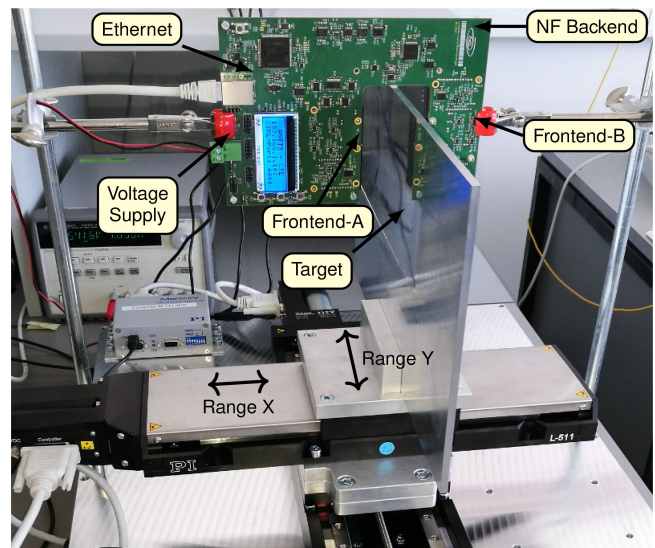


**FIGURE 10.** Photograph of the measurement system presented in [8].
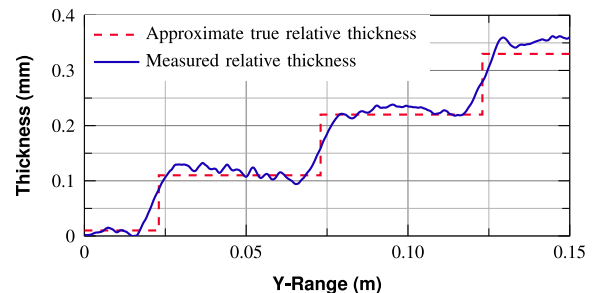


**FIGURE 11.** Measurement results of the system presented in [8].

system operates in the X-band and is based on the evaluation of the reflection coefficient $S_{11}$. As the dielectric constants of the coatings are known, a recalculation algorithm, based on a forward simulation is used to estimate the widths of the dielectric layers [67]. These forward simulations are carried out expecting an ideal conductor as a substrate and it could be shown, that the results are still applicable to real-world substrates such as aluminum or carbon composite. In experiments, relative deviations from the ground truth varying from 8.4% to 15.2% are found. The relative deviations correspond to absolute deviations of 0.45 mm and 0.19 mm, respectively The deviations depend on the complex permittivity and on the coating's thickness. Thicker examples with higher loss and higher permittivity lead to better results in terms of measurement deviation. As it deals with widths of dielectrics, this approach complements the aforementioned approaches for the measurement of conducting materials. The achieved deviations are low enough for the application in industrial environments.

To summarize the three featured approaches for the radar-based sheet thickness measurement, an overview of the key parameters is given in Table 3.

**TABLE 3.** Comparison of the Presented Approaches for Sheet Thickness Monitoring

| Parameter | Reference | | |
|---|---|---|---|
| | [65] | [66] | [8] |
| Frequency (GHz) | 8-10 | 8.2-12.4 | 61 |
| Maximum deviation ($\mu$m) | not stated | 190-450 | $\pm 10$ |
| Typical thickness | arbitrary | several mm | arbitrary |
| Material | metal | dielectric | metal |

## B. SPEED-OVER-GROUND ESTIMATION

The velocity estimation of ground-based vehicles has become an increasingly popular topic in recent years. This is mainly due to the efforts put in automated vehicle technologies for which accurate knowledge of the vehicle's movement is crucial [68]. The utilization of radars for this task suggests itself as radar technology has been used for decades to estimate the position and velocity of various types of targets.

The evaluation of Doppler information from a radar receive signal is probably the best-known approach to estimate the velocity of targets. Accordingly, it is also employed to estimate the speed-over-ground.

In [69] a Doppler-based approach to estimate the full 2D motion state of a vehicle is presented. It makes use of the fact that a vehicle is usually surrounded by numerous stationary targets which can be taken to first estimate the relative velocity vector between each sensor and target. Applying a system model which includes the position and orientation of each sensor at the car, a forward relationship between the vehicle's motion state and the measured target reflections is established. By inverting the system model equation using either a least-squares estimator or orthogonal distance regression, the actual motion state is then estimated. To filter any moving targets the RANdom SAmple Consensus (RANSAC) algorithm is employed [70]. This approach requires the usage of sensors which provide a direction of arrival (DOA) estimation for each target, as the target angles are part of the system model. This system was tested with a vehicle in a parking lot and produces measurement errors well below 0.5% outperforming the standard wheel odometry by a factor of about 3 on average.

A similar approach which does not require any DOA estimation is presented in [71]. It only exploits the range and Doppler information from the environment. The target angles are then estimated using bilateration. This means the range information from two sensors with overlapping field of view are utilized to estimate the angle of a corresponding target. Since this process is ambiguous and therefore leads to ghost targets, this, as well as the problems arising from moving targets, is tackled using the aforementioned RANSAC algorithm. The measurement results for this approach showed an accuracy of about 1.5%. Though, it has to be mentioned that [71] only mentions a single velocity value for the real-world measurement.

Another approach is presented in [72]. It employs a rotating 360° FMCW scanning radar. Using this radar, the system is
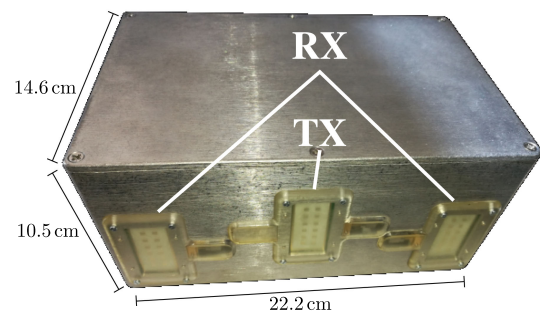


**FIGURE 12.** The field test system presented in [73].

able to extract landmarks from the environment, using a probabilistic filter approach. Subsequent landmark maps are than be compared under rigid transformations to find an optimal match. From the relative movement of the surroundings, the movement of the vehicle itself can be determined with low efforts. This method produced results with a median error of 0.106m s$^{-1}$ during a 10km test drive in a city. The velocity error is therefore comparable to the two previously mentioned methods. Though, the advantage of this method is the resulting map of landmarks which is useful for other processing steps on a vehicle, such as detection and classification of road users. The most significant drawback is likely the need for a rotating radar, which is not common in vehicles.

All the aforementioned approaches use the surroundings of a vehicle to determine the velocity. Another approach is to make use of the ground on which the vehicle is moving. Simple Doppler-based methods which determine the movement relative to the ground often lack accuracy when used on uneven surfaces [74]. More recent approaches which can overcome this issue estimate the speed-over-ground by the usage of correlation based techniques.

In [75]–[77] a down-looking system with two receivers, separated in moving direction, is presented. By correlating both received signals a virtual grating lobe pattern on the ground can be produced. A scatterer passing these lobes creates a harmonic correlation signal whose frequency is proportional to the velocity. The system inherently uses the roughness of the ground which is modeled as a set of individual point scatterers. The unwanted Doppler shifts which are also created by the movement over a rough surface, are then tackled by the use of a neural network. The velocity accuracy achieved with this system is about 0.138m s$^{-1}$ and is therefore in the same order as the former presented approaches. The main feature of this system is the fact that it can be placed underneath the vehicle, a position less prone to being obstructed by snow or other environmental hazards. Also, the computational cost of the processing is rather low.

Another correlation-based approach is introduced in [73]. This system is intended to be used on trains rather than cars. Therefore, only the scalar speed is of interest. The utilized radar system is depicted in Fig. 12 , it consists of two receivers placed next to a transmitter. While the train is moving, both
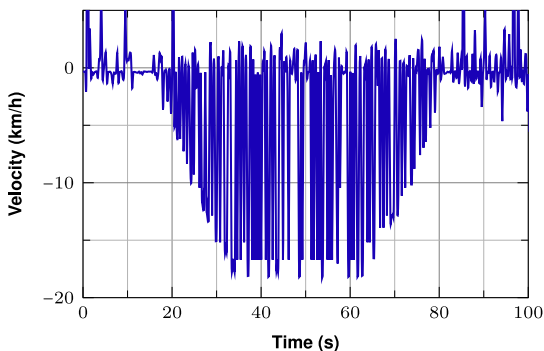
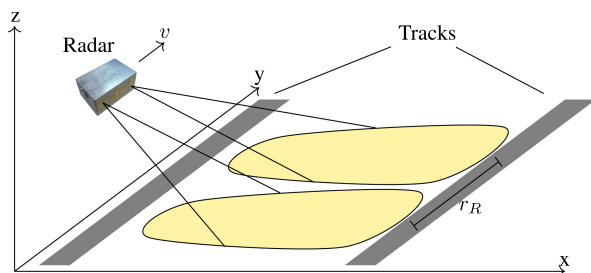**FIGURE 13.** Field test result for the system presented in [73].



**FIGURE 14.** Illustration of the measurement principle presented in [73].

receivers are imaging the track bed as shown in Fig. 14. During processing the cross-correlation sequence of both images is calculated. The peak in the cross-correlation corresponds to the time difference between the two images which is linked to the train's speed. A field test result of this system is depicted in Fig. 13. As can be seen the system suffers from many obvious failed velocity estimations, though the actual velocity is visible as an envelope. This flaw is due to the fact that the angle between transmitter and the respective receiver is not the same, therefore the receivers observe the track bed from different angles. Still, the results give a proof-of-concept and an improved prototype overcoming this issue is already under development.

## C. LOW-POWER APPLICATIONS

In the future the power consumption of planet earth will increase, requiring more energy saving strategies and better system efficiencies. However, since smart factories and smart home applications, as well as different digital consumer goods are flooding the market both statements oppose each other.

As a side-effect of low-power systems, costs are reduced because no wires are needed for the installation of self-sufficient radar-systems. Applications for low-power sensors can be sensors for tank level [78], [79], occupancy and vibration monitoring or even vital sign detection.

To encourage the research in this area a design competition is carried out each year at the International Microwave Symposium (IMS). On the basis of the winning radar system of Lurz *et al.* at the IMS in Honolulu, Hawaii, in 2017, the principle of low-power Doppler radar systems is explained
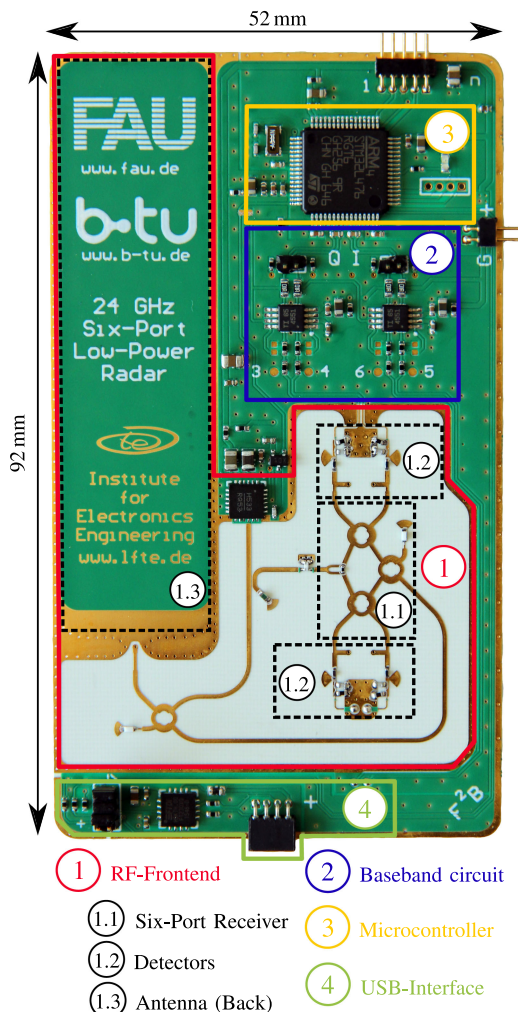


**FIGURE 15.** Photograph of the low-power radar system featured in [25].

[25]. This system showed an average power consumption of less than 30 $\mu$W with a duty-cycling approach of six measurements per second. As a consequence the radar-system could be powered with a CR2032 battery for up to 2 years.

The top side of the realized system is depicted in Fig. 15. In order to reduce the weight as far as possible only a two-layer PCB is used, where the antenna is placed on the back. The system features a VCO for the 24 GHz ISM band as transmitter and a six-port as receiver, whose big advantage is played out in low-power applications. This means that due to its passive structure no power supply is necessary. Furthermore, by using four lumped diode detectors the structure is capable to convert very short RF pulses into a differential pair of I/Q signals. As a consequence, all necessary information of the phase shift and relative displacement is provided by the system.

To achieve this ultra low current consumption of 8.4 $\mu$A the technique of duty-cycling is used. This means that for each measurement, the microcontroller first wakes up from its sleep-mode. Afterwards, all active components are powered up in a defined order and an RF pulse is transmitted. In the next step, the downconverted DC voltages are sampled with
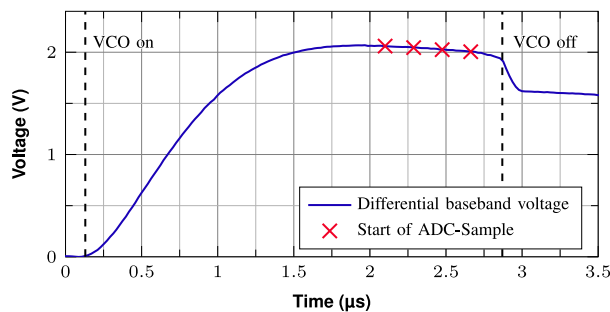
**FIGURE 16.** Measurement of one differential baseband voltage.



**FIGURE 17.** Setup of the vibration measurement with a fan leading to the vibration spectrum shown in Fig. 18.

the internal ADCs and the data is sent to the host via an universal asynchronous receiver transmitter (UART) interface. At the end of the measurement period all active elements are shut down and the microcontroller enters the sleep mode again. The wake-up is triggered by an internal low-power timer.

An exemplary downconverted RF pulse is shown by the recorded differential baseband voltage in Fig. 16. It can be seen that the pulse is less than $3\,\mu$s long and needs about $1.5\,\mu$s to settle, which is caused by the used bandwidth of the baseband filter. Here the trade-off between bandwidth and pulse width becomes obvious. A shorter pulse would reduce the overall current consumption but also enforces a lower bandwidth, leading to a in higher noise floor and a loss of precision. As shown in Fig. 16 the authors of [25] used the implemented quadruple hardware oversampling at each pulse to improve the SNR by still using a lower bandwidth than necessary.

Furthermore, the number of samples per second has to be adjusted to the expected target moving speed or vibration frequency. In this case the Nyquist theorem must still be fulfilled. During the scenario of the competition, target moving frequencies of up to 0.9 Hz were expected. This lead the authors to the usage of a sampling rate of 6 Sps to even measure possible harmonics. During the competition a sensitivity of $100\,\mu$m was demonstrated for a target in 1 m distance.

Concluding this application it becomes obvious that the six-port is well suited for low-power radar applications since less amplification is necessary and a fully passive detection can be used. Due to this, the six-port technology clearly surpasses conventional mixer architectures in term of power added efficiency (PAE).

### D. VIBRATION MONITORING

In many industrial areas, the tracking of a machine's vibration spectrum can prevent high costs due to unexpected failure. It was shown that based on their vibration spectrum e-drives can be monitored to prevent faults [80]–[83]. A fault is not only detected but it can be even further specified. For example, broken bearings, misaligned shafts or rotor bows are detected by investigating the frequency spectrum. By also analyzing the amplitudes of the vibrations the error can be refined more precisely [82]. This in-situ surveillance is called predictive maintenance and reduces the costs and increases safety during
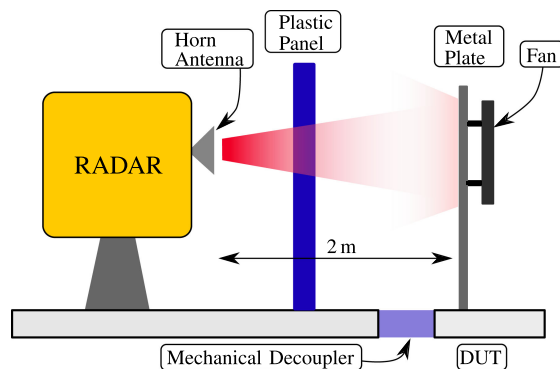
a fault. Usually, this vibration monitoring is done by laser interferometry or piezoelectric sensors. However, the first is comparably expensive and susceptible to fog, dust and dirt whereas the latter cannot be applied remotely.

By using high resolution Doppler-based radar systems both drawbacks can be eliminated since it is possible to measure the spectrum of mechanical vibrations of different machines or even buildings like bridges remotely. The feasibility has been shown in various publications [9], [10], [56], [84]–[87]. Furthermore, radar is capable to penetrate different non conducting materials, that can be used as housings of the radar system. Usually, for simulation of high vibration frequencies speakers or fans are commonly used as DUTs. For the evaluation of low vibration frequencies however, linear stages often serve as targets in order to exactly adjust its amplitudes and frequencies.

In the following part of this subsection a closer look is taken of the publication of Vinci *et al.* in 2013 as an example for radar-based vibration monitoring [9]. Here a six-port radar in the 24 GHz ISM band was used. An overview of the setup is depicted in Fig. 17. The radar system illuminates a metal plate, where a fan is fixed on the opposing side. This fan is realized by a cooler fan with a diameter of 12 cm and a rotation frequency of 36 Hz which corresponds to a rotation speed of 2,160 rounds per minute. Vibrations of the fan are directly transmitted to the metal plate and can be detected by the radar. Together with the metal plate, the fan setup is labeled as DUT and emulates a machine that has to be monitored remotely in an industrial environment. The DUT is mechanically decoupled in order to prevent vibrations which might be transmitted to the radar and reduce the system performance by adding further multiple resonant modes to the vibration spectrum due to its mechanic properties.

On the side of the radar system, a plastic panel (polypropylene) is introduced between the applied horn antenna, featuring a gain of 20 dBi, and the target. This adds the possibility to demonstrate the big advantage in compared to laser vibration measurement systems. In case of the radar sensor, no line of sight is required and housings, fog or dirt do not impair the results.
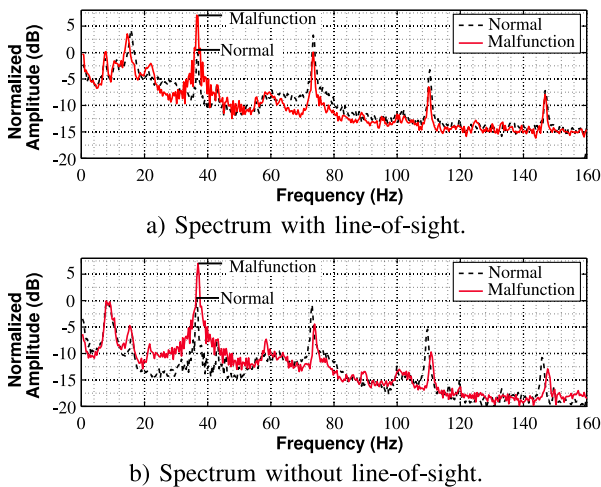
a) Spectrum with line-of-sight.



b) Spectrum without line-of-sight.

**FIGURE 18.** Results of the radar-based vibration measurement presented in [9] in LOS and NLOS in normal operation mode and with introduced malfunctions.



**FIGURE 19.** Possible application of a vital sign sensing radar underneath a patient bed in hospital [89].

To illustrate the systems capabilities during industrial scenarios a measurement was performed under normal and malfunction condition, each in a line of sight (LOS) and non line of sight (NLOS) setup. The malfunction was simulated by attaching a piece of plastic, weighing only 147 mg on one blade of the fan at a distance of 47 mm away from the center point. The measurement data was recorded and an FFT is applied on the acquired data of the relative displacement. The spectra, that are normalized to the maximal value during normal operation of the fan's rotation frequency are depicted in Fig. 18. By comparing the measurements with and without line-of-sight shows that no shift of the fundamental vibration frequency and its harmonics can be seen. Even though almost no frequency shift between normal and malfunction mode occurs, it is obvious that the attachment of the plastic piece strongly increased the amplitude of the fundamental vibration frequency. This shows that in an industrial scenario a fault could have been detected clearly and that radar technology is more than an alternative for predictive maintenance of e-drives or heavy machines.

### E. VITAL SIGN SENSING

A special measurement application related to vibration monitoring is the sensing of the signs of life. Both humans and animals show inevitable vibrations of their skin due to body movement, heart beat, and respiration when they are alive - and these can be captured by radar systems. This creates potential applications in the medical field, to objectively evaluate patients' health state and to track the process of recovery. A big advantage over conventional measurement devices, such as the electrocardiogram (ECG) or the photoplethysmogram (PPG) is the ability to acquire the data without requiring contact to the patient. Even clothing and mattress are penetrated by microwaves and millimeter waves under normal circumstances. This enables a long-time monitoring without causing
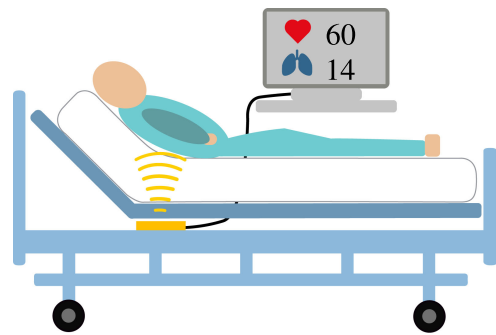
stress or reducing the patients' comfort [88]. An example for a vital sign radar included in a patient bed can be seen in Fig. 19.

Typical system prototypes use operating frequencies in the range of 1 GHz [90] up to 300 GHz [91], with a clear focus on the microwave and millimeter-wave ISM bands. In applications where only a single subject is supposed to be monitored, the unmodulated CW radar is oftentimes preferred over FMCW radar due to its high phase resolution at a low system complexity [92]. Because the biological signals are only slow-varying, a measurement bandwidth of about 100 Hz is sufficient to capture respiration and heart beat [93]. The low bandwidth helps to reduce noise and high-resolution ADCs are available to reduce quantization noise, leading in sum to a low RMS error of the distance measurement. Depending on the spot on the body illuminated by the antenna, the distance signal contains different information: First, the chest displacement due to respiration, which can be used to determine the number of breaths per minute [94]. Second, the contraction and expansion of heart or the resulting change in diameter of large blood vessels. This can be used to estimate the heart rate [93], to assess the shape of the pulse wave [95] or to measure its transit time, the so-called pulse wave velocity, which contains information on the state of the vessels' walls [96], [97]. An exemplary signal measured with a 24 GHz CW radar is shown in fig. 20. The third vital signal, which can be captured by high-precision radar systems, are the vibrations of the chest caused by the closure of heart valves, which are contained in the so-called apex cardiogram [98] (see Fig. 20). These prominent heart sounds, which are usually transformed into audible sound by a stethoscope, can be used to precisely determine the inter-beat-intervals, and the resulting heart rate variability, which is related to the autonomous nervous system and hence can indicate stress, relaxation, or several diseases [93], [99]. Typical amplitudes and frequencies of all three signal components are listed in Table 4. The current challenge is to develop sensors which a sufficiently large dynamic range on the one hand, and on the other to create algorithms for the extraction of the relevant features from the raw distance measurement.

In addition to the monitoring of patients in hospital, sensors for the surveillance at home, in office or in vehicles are
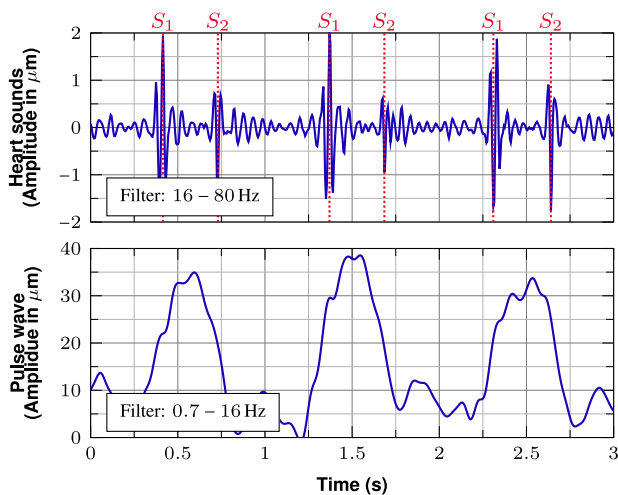
**FIGURE 20. Cardiac action recorded with a CW radar system focusing on the human chest.**

**TABLE 4. Approximate Amplitudes and Frequency Bands of Healthy Humans' Vital Parameters in Resting Condition**

|  | Amplitudes (pk-pk) | Spectral band |
|---|---|---|
| Respiration [94] | $5-20\,\text{mm}$ | $0.03-0.5\,\text{Hz}$ |
| Pulse wave [95] | $100-500\,\mu\text{m}$ | $0.67-15\,\text{Hz}$ |
| Heart sounds [99] | $1-50\,\mu\text{m}$ | $16-80\,\text{Hz}$ |

another big field of application. Especially persons at risk, such as elderly or sick can benefit from a continuous monitoring. In these scenarios, additional features like for instance a fall detection often require an angular resolution [100]. If entire rooms are to be covered by a monitoring system, the complex measurement scenarios usually require modulated signals, such as FMCW radar [101], [102]. In combination with analog or digital beamforming techniques, this adds the ability to separate targets in angle and distance, and to record the vital signs of more than one person at a time.

In addition to a continuous vital sign monitoring for diagnostic purposes, detecting any vital signs, such as body movements in debris after earthquakes is an important field of research as well. In these cases, UWB radar is frequently used due to its spread spectrum and the resulting robustness and improved penetration of dielectric obstacles [103]–[105].

Not only the vital signs of humans are of interest. Recently, radar systems have also been proposed for the application in livestock farming. In [106], an UWB radar has been used to monitor heart and respiration rate of cows. Moreover, a FMCW radar was used by [107], [108] to detect anomalies in the gait of sheep and cows as an indication of lameness. Thus radar sensors can also be used to optimize modern farming by detecting and preventing diseases of the livestock.

## V. CONCLUSION

It can be stated that radar systems have made their way into various industries and also into our daily life. Due to recent advances regarding technology, system design and signal processing, the systems can be adapted to measurement tasks from the sub-micrometer range to hundreds of kilometers. Due to their ability to penetrate many dielectric materials and hence to perform a contactless measurement of distance, vibration, and even vital parameters without causing harm to humans, they will more and more supplement or even substitute conventional cable-based sensors in the near future. Their application increases production efficiencies, improves quality and hence and reduces the prize of goods. Moreover, the risk of injuries and accidents can be lowered, even vital parameters of humans and animals can be tracked for diagnostic or therapeutic reasons. All of these benefits are a great motivation for engineers to keep pushing the limits of radar systems. In particular, miniaturization is a big topic of interest, where bridging the gap between the microwave and the optical frequency ranges offer new material-to-waves physics interactions to foresee novel applications. The development of flexible RF materials leads to systems which can be mounted on almost any surface. Moreover, advances in the 3D printing of circuits and components offers a rapid prototyping and a accelerates the development process. Finally, the use of biomaterials enables the design of eco-friendly radars. Upcoming circuit technologies support this by promising a lower power consumption to increase efficiency.

## REFERENCES

[1] T. K. Sarkar, M. Salazar Palma, and E. L. Mokole, "Echoing across the years: A history of early radar evolution," *IEEE Microw. Mag.*, vol. 17, no. 10, pp. 46–60, Oct. 2016.

[2] M. Vogt and M. Gerding, "Silo and tank vision: Applications, challenges, and technical solutions for radar measurement of liquids and bulk solids in tanks and silos," *IEEE Microw. Mag.*, vol. 18, no. 6, pp. 38–51, Sep./Oct. 2017.

[3] M. Vogt, "Radar sensors (24 and 80 GHz range) for level measurement in industrial processes," in *Proc. IEEE MTT-S Int. Conf. Microw. Intell. Mobility*, 2018, pp. 1–4.

[4] A. Kaineder, C. Michenthaler, D. Hammerschmidt, and A. Stelzer, "Guided wave tank level sensor," in *Proc. 16th Eur. Radar Conf.*, 2019, pp. 301–304.

[5] S. Ayhan, S. Scherr, P. Pahl, T. Kayser, M. Pauli, and T. Zwick, "High-accuracy range detection radar sensor for hydraulic cylinders," *IEEE Sensors J.*, vol. 14, no. 3, pp. 734–746, Mar. 2014.

[6] S. Ayhan, S. Scherr, M. Pauli, and T. Zwick, "FMCW radar in oil-filled waveguides for range detection in hydraulic cylinders," in *Proc. 9th Eur. Radar Conf.*, 2012, pp. 63–66.

[7] S. Lindner, F. Barbon, S. Linz, S. Mann, R. Weigel, and A. Koelpin, "Distance measurements based on guided wave 24 GHz dual tone six-port radar," in *Proc. 11th Eur. Radar Conf.*, 2014, pp. 57–60.

[8] S. Mann *et al.*, "High-precision interferometric radar for sheet thickness monitoring," *IEEE Trans. Microw. Theory Techn.*, vol. 66, no. 6, pp. 3153–3166, Jun. 2018.

[9] G. Vinci *et al.*, "Six-Port microwave interferometer radar for mechanical vibration analysis," in *Proc. Eur. Microw. Conf.*, 2013, pp. 1599–1602.

[10] Y. Yan, C. Li, J. A. Rice, and J. Lin, "Wavelength division sensing RF vibrometer," in *Proc. IEEE MTT-S Int. Microw. Symp.*, 2011, pp. 1–4.

[11] C. Gu and J. Lien, "A two-tone radar sensor for concurrent detection of absolute distance and relative movement for gesture sensing," *IEEE Sensors Lett.*, vol. 1, no. 3, pp. 1–4, Jun. 2017.

[12] S. Lindner, F. Barbon, S. Mann, G. Vinci, R. Weigel, and A. Koelpin, "Dual tone approach for unambiguous six-port based interferometric distance measurements," in *IEEE MTT-S Int. Microw. Symp. Dig.*, 2013, pp. 1–4.

[13] J. Wang, T. Karp, J.-M. Munoz-Ferreras, R. Gomez-Garcia, and C. Li, "A spectrum-efficient FSK radar technology for range tracking of both moving and stationary human subjects," *IEEE Trans. Microw. Theory Techn.*, vol. 67, no. 12, pp. 5406–5416, Dec. 2019.

[14] K. Statnikov, N. Sarmah, J. Grzyb, S. Malz, B. Heinemann, and U. R. Pfeiffer, "A 240 GHz circular polarized FMCW radar based on a SiGe transceiver with a lens-integrated on-chip antenna," in *Proc. 11th Eur. Radar Conf.*, 2014, pp. 447–450.

[15] T. Jaeschke, C. Bredendiek, and N. Pohl, "A 240 GHz ultra-wideband FMCW radar system with on-chip antennas for high resolution radar imaging," in *IEEE MTT-S Int. Microw. Symp. Dig.*, 2013, pp. 1–4.

[16] N. Pohl *et al.*, "Radar measurements with micrometer accuracy and nanometer stability using an ultra-wideband 80 GHz radar system," in *Proc. IEEE Top. Conf. Wireless Sensors Sensor Netw.*, 2013, pp. 31–33.

[17] T. Jaeschke, C. Bredendiek, S. Kuppers, and N. Pohl, "High-PRECISIOn D-Band FMCW-radar sensor based on a wideband SiGe-transceiver MMIC," *IEEE Trans. Microw. Theory Techn.*, vol. 62, no. 12, pp. 3582–3597, Dec. 2014.

[18] I. I. Immoreev and P. G. S. D. V. Fedotov, "Ultra wideband radar systems: Advantages and disadvantages," in *Proc. IEEE Conf. Ultra Wideband Syst. Technol.*, 2002, pp. 201–205.

[19] H. J. Ng, M. Kucharski, and D. Kissinger, "Pseudo-random noise radar for short-range applications in SiGe technologies," in *Proc. 22nd Int. Microw. Radar Conf.*, 2018, pp. 338–341.

[20] A. Lazaro, D. Girbau, R. Villarino, and A. Ramos, "Vital signs monitoring using impulse based UWB signal," in *Proc. 41st Eur. Microw. Conf.*, 2011, pp. 135–138.

[21] R. Sorrentino and G. Bianchi, *Microwave and RF Engineering*, 2nd ed. (Microwave and Optical Engineering). Hoboken, NJ, USA: Wiley, 2010, vol. v.2.

[22] L. Piotrowsky, T. Jaeschke, S. Kueppers, J. Siska, and N. Pohl, "Enabling high accuracy distance measurements with FMCW radar sensors," *IEEE Trans. Microw. Theory Techn.*, vol. 67, no. 12, pp. 5360–5371, Dec. 2019.

[23] C. A. Balanis, *Antenna Theory: Analysis and Design*, 4th ed. Hoboken, New York, NY, USA: Wiley, 2016.

[24] International Telecommunication Union, "2016 Radio Regulations: Volume 1," 2016. [Online]. Available: http://handle.itu.int/11.1002/pub/80da2b36-en

[25] F. Lurz, F. Michler, B. Scheiner, R. Weigel, and A. Koelpin, "Microw(h)att?! Ultralow-power six-port radar: Realizing highly integrated portable radar systems with good motion sensitivity at relatively low cost," *IEEE Microw. Mag.*, vol. 19, no. 1, pp. 91–98, Jan. 2018.

[26] M. C. Budge and M. P. Burt, "Range correlation effects in radars," in *Proc. Rec. IEEE Nat. Radar Conf.*, 1993, pp. 212–216.

[27] S. Lindner, F. Barbon, S. Linz, S. Mann, R. Weigel, and A. Koelpin, "Distance measurements and limitations based on guided wave 24 GHz dual tone six-port radar," *Int. J. Microw. Wireless Technol.*, vol. 7, no. 3-4, pp. 425–432, Jun. 2015.

[28] S. Mann, F. Lurz, R. Weigel, and A. Koelpin, "A high-sensitivity radar system featuring low weight and power consumption," *IEEE Microw. Mag.*, vol. 16, no. 2, pp. 99–105, Mar. 2015.

[29] S. Thomas, C. Bredendiek, and N. Pohl, "A SiGe-based 240-GHz FMCW radar system for high-resolution measurements," *IEEE Trans. Microw. Theory Techn.*, vol. 67, no. 11, pp. 4599–4609, Nov. 2019.

[30] W. Winkler, W. Debski, D. Genschow, and R. Kraemer, "24 GHz transceiver front-end with two RX-channels," in *Proc. German Microw. Conf.*, 2015, pp. 1–4.

[31] C. Beck *et al.*, "Industrial mmWave radar sensor in embedded wafer-level BGA packaging technology," *IEEE Sensors J.*, vol. 16, no. 17, pp. 6566–6578, Sep. 2016.

[32] G. F. Engen and C. A. Hoer, "Application of an arbitrary 6-port junction to power-measurement problems," *IEEE Trans. Instrum. Meas.*, vol. 21, no. 4, pp. 470–474, Nov. 1972.

[33] J. Li, R. G. Bosisio, and K. Wu, "A six-port direct digital millimeter wave receiver," in *IEEE MTT-S Int. Microw. Symp. Dig.*, 1994, pp. 1659–1662.

[34] J. Li, R. G. Bosisio, and K. Wu, "Computer and measurement simulation of a new digital receiver operating directly at millimeter-wave frequencies," *IEEE Trans. Microw. Theory Techn.*, vol. 43, no. 12, pp. 2766–2772, Dec. 1995.

[35] S. O. Tatu, E. Moldovan, G. Brehm, K. Wu, and R. G. Bosisio, "Ka-band direct digital receiver," *IEEE Trans. Microw. Theory Techn.*, vol. 50, no. 11, pp. 2436–2442, Nov. 2002.

[36] Y. Zhao, C. Viereck, J. F. Frigon, R. G. Bosisio, and K. Wu, "Direct quadrature phase shift keying modulator using six-port technology," *Electron. Lett.*, vol. 41, no. 21, pp. 1180–1181, Oct. 2005.

[37] Y. Zhao, J. F. Frigon, K. Wu, and R. G. Bosisio, "Multi(six)-port impulse radio for ultra-wideband," *IEEE Trans. Microw. Theory Techn.*, vol. 54, no. 4, pp. 1707–1712, Jun. 2006.

[38] E. Moldovan, S. O. Tatu, T. Gaman, K. Wu, and R. G. Bosisio, "A new 94-GHz six-port collision-avoidance radar sensor," *IEEE Trans. Microw. Theory Techn.*, vol. 52, no. 3, pp. 751–759, Mar. 2004.

[39] E. Moldovan, S. O. Tatu, S. Affes, R. G. Bosisio, and Ke Wu, "W-band substrate integrated waveguide radar sensor based on multi-port technology," in *Proc. Eur. Microw. Conf.*, 2007, pp. 1453–1456.

[40] A. Koelpin, F. Lurz, S. Linz, S. Mann, C. Will, and S. Lindner, "Six-port based interferometry for precise radar and sensing applications," *Sensors (Basel, Switzerland)*, vol. 16, no. 10, 2016, Art. no. 1556.

[41] M. N. Solomon, P. S. Weitzman, C. P. McClay, and H. M. Cronson, "A monolithic six-port module," *IEEE Microw. Guided Wave Lett.*, vol. 2, no. 8, pp. 334–336, Aug. 1992.

[42] S. O. Tatu, E. Moldovan, K. Wu, and R. G. Bosisio, "A new direct millimeter-wave six-port receiver," *IEEE Trans. Microw. Theory Techn.*, vol. 49, no. 12, pp. 2517–2522, Dec. 2001.

[43] B. Laemmle *et al.*, "A fully integrated 120-GHz six-port receiver front-end in a 130-nm SiGe BiCMOS technology," in *Proc. IEEE 13th Top. Meet. Silicon Monolithic Integr. Circuits RF Syst.*, 2013, pp. 129–131.

[44] C. Gu, Y. He, and J. Zhu, "Noncontact vital sensing with a miniaturized 2.4 GHz circularly polarized Doppler radar," *IEEE Sensors Lett.*, vol. 3, no. 7, pp. 1–4, Jul. 2019.

[45] G. Armbrecht, E. Denicke, N. Pohl, T. Musch, and I. Rolfes, "Compact directional UWB antenna with dielectric insert for radar distance measurements," in *Proc. IEEE Int. Conf. Ultra-Wideband*, 2008, pp. 229–232.

[46] B. Scheiner, F. Michler, F. Lurz, R. Weigel, and A. Koelpin, "Nothing beats SNR: Single-digit micrometer ranging using a low-power CW radar featuring a low-weight 3D-printed horn antenna," *IEEE Microw. Mag.*, vol. 21, no. 1, pp. 88–95, Jan. 2020.

[47] C. Bredendiek, N. Pohl, T. Jaeschke, K. Aufinger, and A. Bilgic, "A 240 GHz single-chip radar transceiver in a SiGe bipolar technology with on-chip antennas and ultra-wide tuning range," in *Proc. IEEE Radio Freq. Integr. Circuits Symp.*, 2013, pp. 309–312.

[48] T.-Y. J. Kao, Y. Yan, T.-M. Shen, A. Y.-K. Chen, and J. Lin, "Design and analysis of a 60-GHz CMOS Doppler micro-radar system-in-package for vital-sign and vibration detection," *IEEE Trans. Microw. Theory Techn.*, vol. 61, no. 4, pp. 1649–1659, Apr. 2013.

[49] M. Frank, F. Lurz, R. Weigel, and A. Koelpin, "Compact low-cost substrate integrated waveguide fed antenna for 122 GHz radar applications," *Int. J. Microw. Wireless Technol.*, vol. 11, no. 4, pp. 408–412, May 2019.

[50] E. Hassan *et al.*, "Multilayer topology optimization of wideband SIW-to-waveguide transitions," *IEEE Trans. Microw. Theory Techn.*, vol. 68, no. 4, pp. 1326–1339, Apr. 2020.

[51] S. Yoo, Y. Milyakh, H. Kim, C. Hong, and H. Choo, "Patch array antenna using a dual coupled feeding structure for 79 GHz automotive radar applications," *IEEE Antennas Wireless Propag. Lett.*, vol. 19, no. 4, pp. 676–679, Apr. 2020.

[52] P. Hallbjorner, Z. He, S. Bruce, and S. Cheng, "Low-profile 77-GHz lens antenna with array feeder," *IEEE Antennas Wireless Propag. Lett.*, vol. 11, pp. 205–207, Feb. 2012.

[53] E. Ozturk *et al.*, "A 120 GHz SiGe BiCMOS monostatic transceiver for radar applications," in *Proc. 13th Eur. Microw. Integr. Circuits Conf.*, 2018, pp. 41–44.

[54] W. Ser, J. Yu, X. Guo, J. Zhang, and M. E. H. Ong, "Noncontact heart rate measurement using a 24 GHz Doppler radar," in *Proc. Microw. Workshop Series RF Wireless Technol. Biomed. Healthcare Appl.*, 2013, pp. 1–3.

[55] H.-C. Kuo, C.-C. Chou, C.-C. Lin, C.-H. Yu, T.-H. Huang, and H.-R. Chuang, "A 60-GHz CMOS direct-conversion Doppler radar RF sensor with clutter canceller for single-antenna noncontact human vital-signs detection," in *Proc. Radio Freq. Integr. Circuits Symp.*, 2015, pp. 35–38.

[56] S. Bera, M. Das, T. Singh, and R. Bera, "Implementation of adaptive 24 GHz Doppler radar," in *Proc. URSI Asia-Pacific Radio Sci. Conf.*, 2019, pp. 1–4.

[57] X. Ma, Y. Wang, W. Song, X. You, J. Lin, and L. Li, "A 100-GHz double-sideband low-if CW Doppler radar in 65-nm CMOS for mechanical vibration and biological vital sign detections," in *Proc. IEEE MTT-S Int. Microw. Biomed. Conf.*, 2019, pp. 136–139.

[58] P. K. Gogoi, M. K. Mandal, A. Kumar, and T. Chakravarty, "A 2.4 GHz compact Doppler radar module for vibration monitoring," in *Proc. IEEE MTT-S Int. Microw. RF Conf.*, 2019, pp. 1–4.

[59] Y. Xiao, J. Lin, O. Boric-Lubecke, and M. Lubecke, "Frequency-tuning technique for remote detection of heartbeat and respiration using low-power double-sideband transmission in the Ka-band," *IEEE Trans. Microw. Theory Techn.*, vol. 54, no. 5, pp. 2023–2032, May 2006.

[60] A. Singh *et al.*, "Data-based quadrature imbalance compensation for a CW Doppler radar system," *IEEE Trans. Microw. Theory Techn.*, vol. 61, no. 4, pp. 1718–1724, Apr. 2013.

[61] M. Zakrzewski *et al.*, "Quadrature imbalance compensation with ellipse-fitting methods for microwave radar physiological sensing," *IEEE Trans. Microw. Theory Techn.*, vol. 62, no. 6, pp. 1400–1408, Jun. 2014.

[62] S. Linz, F. Lurz, R. Weigel, and A. Koelpin, "Extended ellipse-based reconstruction algorithm for six-port radar," in *Proc. IEEE Radio Wireless Symp.*, 2019, pp. 1–3.

[63] S. Linz *et al.*, "I/Q imbalance compensation for Six-port interferometers in radar applications," in *Proc. 44th Eur. Microw. Conf.*, 2014, pp. 746–749.

[64] A. Kugi, W. Haas, K. Schlacher, K. Aistleitner, H. M. Frank, and G. W. Rigler, "Active compensation of roll eccentricity in rolling mills," *IEEE Trans. Ind. Appl.*, vol. 36, no. 2, pp. 625–632, Mar./Apr. 2000.

[65] K. Hoffmann and Z. Skvor, "Microwave interferometric method for metal sheet thickness measurement," in *Proc. IEEE 81st Microw. Meas. Conf.*, 2013, pp. 1–3.

[66] R. Zoughi, J. R. Gallion, and M. T. Ghasr, "Accurate microwave measurement of coating thickness on carbon composite substrates," *IEEE Trans. Instrum. Meas.*, vol. 65, no. 4, pp. 951–953, Apr. 2016.

[67] M. T. Ghasr, D. Simms, and R. Zoughi, "Multimodal solution for a waveguide radiating into multilayered structures—Dielectric property and thickness evaluation," *IEEE Trans. Instrum. Meas.*, vol. 58, no. 5, pp. 1505–1513, May 2009.

[68] X. Jin, G. Yin, and N. Chen, "Advanced estimation techniques for vehicle system dynamic state: A survey," *Sensors (Basel, Switzerland)*, vol. 19, no. 19, 2019, Art. no. 4289.

[69] D. Kellner, M. Barjenbruch, J. Klappstein, J. Dickmann, and K. Dietmayer, "Instantaneous ego-motion estimation using multiple Doppler radars," in *Proc. IEEE Int. Conf. Robot. Autom.*, 2014, pp. 1592–1597.

[70] M. A. Fischler and R. C. Bolles, "Random sample consensus: A paradigm for model fitting with applications to image analysis and automated cartography," *Commun. ACM*, vol. 24, no. 6, pp. 381–395, Jun. 1981.

[71] M. Steiner, O. Hammouda, and C. Waldschmidt, "Ego-Motion estimation using distributed single-channel radar sensors," in *Proc. IEEE MTT-S Int. Conf. Microwav. Intell. Mobility*, 2018, pp. 1–4.

[72] S. H. Cen and P. Newman, "Precise ego-motion estimation with millimeter-wave radar under diverse and challenging conditions," in *Proc. IEEE Int. Conf. Robot. Autom.*, 2018, pp. 1–8.

[73] T. Reissland, B. Lenhart, J. Lichtblau, M. Sporer, R. Weigel, and A. Koelpin, "Evaluation of a robust correlation-based true-speed-over-ground measurement system employing a FMCW radar," in *Proc. Int. J. Microw. Wireless Technol.*, vol. 11, no. 7, pp. 686–693, Sep. 2019.

[74] K. K. M. Shariff, Z. Awang, I. Pasya, and S. A. M. Al Junid, "Theoretical accuracy analysis of a 4-beam speed-over-ground radar on uneven surface," in *Proc. IEEE Int. RF Microw. Conf.*, 2018, pp. 325–328.

[75] J. A. Nanzer, "Millimeter-wave interferometric angular velocity detection," *IEEE Trans. Microw. Theory Techn.*, vol. 58, no. 12, pp. 4128–4136, Dec. 2010.

[76] E. Klinefelter and J. A. Nanzer, "Velocity estimation with a distributed array for autonomous ground vehicles," in *Proc. IEEE MTT-S Int. Conf. Microw. Intell. Mobility*, 2019, pp. 1–3.

[77] E. Klinefelter and J. A. Nanzer, "Interferometric microwave radar with a feedforward neural network for vehicle speed-over-ground estimation," *IEEE Microw. Wireless Compon. Lett.*, vol. 30, no. 3, pp. 304–307, Mar. 2020.

[78] S. Heining *et al.*, "An ultra broadband multi-tone six-port radar for distance measurements in K-Band waveguides," in *Proc. IEEE Radio Wireless Symp.*, 2020, pp. 279–282.

[79] B. Scheiner, F. Lurz, F. Michler, S. Linz, R. Weigel, and A. Koelpin, "Six-port based multitone and low-power radar system for waveguide measurements in smart factories," in *Proc. IEEE 48th Eur. Microw. Conf.*, 2018, pp. 1065–1068.

[80] R. O. Eis, "Electric motor vibration-cause, prevention, and cure," *IEEE Trans. Ind. Appl.*, vol. IA-11, no. 3, pp. 267–275, May 1975.

[81] E. Hashish, K. Miller, W. Finley, and S. Kreitzer, "Vibration diagnostic challenges in electric motor applications," in *Proc. IEEE Petroleum Chem. Ind. Tech. Conf.*, 2015, pp. 1–12.

[82] E. Hashish, K. Miller, W. Finley, and S. Kreitzer, "Vibration diagnostic challenges: Case studies in electric motor applications," *IEEE Ind. Appl. Mag.*, vol. 23, no. 4, pp. 22–34, Aug. 2017.

[83] W. R. Finley, M. M. Hodowanec, and W. G. Holter, "An analytical approach to solving motor vibration problems," *IEEE Trans. Ind. Appl.*, vol. 36, no. 5, pp. 1467–1480, Sep./Oct. 2000.

[84] F. Barbon, G. Vinci, S. Lindner, R. Weigel, and A. Koelpin, "A six-port interferometer based micrometer-accuracy displacement and vibration measurement radar," in *Proc. IEEE MTT-S Int. Microw. Symp.*, 2012, pp. 1–3.

[85] A. Raffo, S. Costanzo, and G. Di Massa, "Software defined Doppler radar as a contactless multipurpose microwave sensor for vibrations monitoring," *Sensors (Basel, Switzerland)*, vol. 17, no. 1, 2017, Art. no. 115.

[86] R. Rakshit, D. Roy, and T. Chakravarty, "On characterization of vibration measurement using microwave Doppler radar," in *Proc. IEEE SENSORS*, 2018, pp. 1–4.

[87] J. Wang, X. Wang, L. Chen, J. Huangfu, C. Li, and L. Ran, "Non-contact distance and amplitude-independent vibration measurement based on an extended DACM algorithm," *IEEE Trans. Instrum. Meas.*, vol. 63, no. 1, pp. 145–153, Jan. 2014.

[88] H. Hong *et al.*, "Microwave sensing and sleep: Noncontact sleep-monitoring technology with microwave biomedical radar," *IEEE Microw. Mag.*, vol. 20, no. 8, pp. 18–29, Aug. 2019.

[89] F. Michler *et al.*, "A radar-based vital sign sensing system for in-bed monitoring in clinical applications," in *Proc. German Microw. Conf.*, 2020, pp. 188–191.

[90] J.-H. Park, Y.-J. Jeong, G.-E. Lee, J.-T. Oh, and J.-R. Yang, "915-MHz continuous-wave Doppler radar sensor for detection of vital signs," *Electronics*, vol. 8, no. 5, p. 561, 2019. [Online]. Available: https://www.mdpi.com/2079-9292/8/5/561

[91] M. Caris *et al.*, "Very high resolution radar at 300 GHz," in *Proc. 11th Eur. Radar Conf.*, 2014, pp. 494–496.

[92] C. Li, V. M. Lubecke, O. Boric-Lubecke, and J. Lin, "A review on recent advances in Doppler radar sensors for noncontact healthcare monitoring," *IEEE Trans. Microw. Theory Techn.*, vol. 61, no. 5, pp. 2046–2060, May 2013.

[93] F. Michler *et al.*, "A clinically evaluated interferometric continuous-wave radar system for the contactless measurement of human vital parameters," *Sensors (Basel, Switzerland)*, vol. 19, no. 11, 2019, Art. no. 2492.

[94] C. Gu *et al.*, "Accurate respiration measurement using DC-coupled continuous-wave radar sensor for motion-adaptive cancer radiotherapy," *IEEE Trans. Biomed. Eng.*, vol. 59, no. 11, pp. 3117–3123, Nov. 2012.

[95] C. Will *et al.*, "Local pulse wave detection using continuous wave radar systems," *IEEE J. Electromagn., RF Microw. Med. Biol.*, vol. 1, no. 2, pp. 81–89, Dec. 2017.

[96] R. Vasireddy, J. Goette, M. Jacomet, and A. Vogt, "Estimation of arterial pulse wave velocity from Doppler radar measurements: A feasibility study," in *Proc. 40th Annu. Int. Conf. IEEE Eng. Med. Biol. Soc.*, 2018, pp. 5460–5464.

[97] F. Michler *et al.*, "Pulse wave velocity detection using a 24 GHz six-port based Doppler radar," in *Proc. IEEE Radio Wireless Symp.*, 2019, pp. 1–3.

[98] J. C. Lin, J. Kiernicki, M. Kiernicki, and P. B. Wollschlaeger, "Microwave apexcardiography," *IEEE Trans. Microw. Theory Techn.*, vol. 27, no. 6, pp. 618–620, Jun. 1979.

[99] C. Will *et al.*, "Radar-based heart sound detection," *Sci. Rep.*, vol. 8, no. 1, 2018, Art. no. 11551.

[100] Z. Peng and C. Li, "Portable microwave radar systems for short-range localization and life tracking: A review," *Sensors (Basel, Switzerland)*, vol. 19, no. 5, 2019, Art. no. 1136.

[101] T. Yang, J. Cao, and Y. Guo, "Placement selection of millimeter wave FMCW radar for indoor fall detection," in *Proc. IEEE MTT-S Int. Wireless Symp.*, 2018, pp. 1–3.

[102] Z. Peng, J. Muñoz-Ferreras, R. Gómez-García, and C. Li, "FMCW radar fall detection based on ISAR processing utilizing the properties of RCS, range, and Doppler," in *Proc. IEEE MTT-S Int. Microw. Symp.*, 2016, pp. 1–3.

[103] K. Wang, Z. Zeng, and J. Sun, "Through-wall detection of the moving paths and vital signs of human beings," *IEEE Geosci. Remote Sens. Lett.*, vol. 16, no. 5, pp. 717–721, May 2019.

[104] L. Ren, Y. S. Koo, H. Wang, Y. Wang, Q. Liu, and A. E. Fathy, "Non-contact multiple heartbeats detection and subject localization using UWB impulse Doppler radar," *IEEE Microw. Wireless Compon. Lett.*, vol. 25, no. 10, pp. 690–692, Oct. 2015.

[105] J. Li, L. Liu, Z. Zeng, and F. Liu, "Advanced signal processing for vital sign extraction with applications in uwb radar detection of trapped victims in complex environments," *IEEE J. Sel. Topics Appl. Earth Observ. Remote Sens.*, vol. 7, no. 3, pp. 783–791, Mar. 2014.

[106] J. Sachs *et al.*, "Remote heartbeat capturing of high yield cows by UWB radar," in *Proc. 16th Int. Radar Symp.*, 2015, pp. 961–966.

[107] F. Fioranelli *et al.*, "Radar-based evaluation of lameness detection in ruminants: Preliminary results," in *Proc. IEEE MTT-S Int. Microw. Biomed. Conf. (IMBioC)*, 2019, pp. 1–4.

[108] A. Shrestha *et al.*, "Animal lameness detection with radar sensing," *IEEE Geosci. Remote Sens. Lett.*, vol. 15, no. 8, pp. 1189–1193, 2018.

**TORSTEN REISSLAND** (Student Member, IEEE) received the B.S. degree in computer engineering from the Ilmenau University of Technology in 2013 and the M.S. in electrical engineering from Friedrich-Alexander University Erlangen-Nuremberg in 2016. In 2016, he joined the Institute for Electronics Engineering, Friedrich-Alexander-University Erlangen-Nuremberg (FAU), as a Research Assistant. His current research interests include signal processing of radar and interferometric systems with focuses on signal modeling and imaging.

**ROBERT WEIGEL** (Fellow, IEEE) is currently a Full Professor with the University of Erlangen-Nuremberg (FAU), Erlangen, Germany. He co-founded several companies in Germany and Austria, where the Austrian company DICE in Linz was split and overtaken by Infineon and Intel, respectively, and Intel sold its company meanwhile to Apple. He has been engaged in research on microwave electronic circuits and systems and has authored or coauthored more than 1200 articles. He was the recipient of the 2002 VDE ITG-Award, the 2007 IEEE Microwave Applications Award, the 2016 IEEE MTT-S Distinguished Educator Award, the 2018 Distinguished Service Award of the EuMA, the 2018 IEEE Rudolf Henning Distinguished Mentoring Award, and the 2020 IEEE Microwave Career Award. He has been a Distinguished Microwave Lecturer, MTT-S AdCom Member, and the 2014 MTT-S President.

**FABIAN MICHLER** (Student Member, IEEE) received the B.S. and M.S. degrees in electrical engineering and communications engineering from Darmstadt University of Technology, Darmstadt, Germany, in 2013 and 2016, respectively. In 2016, he joined the Institute for Electronics Engineering, Friedrich-Alexander-University Erlangen-Nuremberg (FAU), Erlangen, Germany, as a Research Assistant. His current research interests include RF-front ends and microwave circuit design for precise low-power radar systems, particularly for the remote detection of human vital parameters and industrial metering. He is a member of the IEEE Microwave Theory and Techniques Society (IEEE MTT-S). He was the recipient of the First Prize of the Low-Power Radar Student Design Competition of the IEEE International Microwave Symposium in 2017, 2018, and 2019. He is a Co-Founder of the spin-off Sykno, a company for technical consulting and the development of rf sensor systems.

**BENEDICT SCHEINER** (Student Member, IEEE) received the B.S. degree in medical engineering and the M.S. degree in electrical engineering from Friedrich-Alexander-University Erlangen-Nuremberg (FAU), Erlangen, Germany, in 2014 and 2017, respectively. Since 2017, he has been working toward the Ph.D. degree with the Institute for Electronics Engineering, FAU. His research interests focus on system design of different RF sensor systems mainly for industrial applications. He was the recipient of the first place award at the student design competition about radar system design at the IEEE International Microwave Symposium (IMS) in 2017, 2018, and 2019 and won the Graduate Student Challenge at the IMS 2018. Beside his scientific work he is Co-Founder of Sykno, a company for consulting and the design of high frequency sensor systems.

**ALEXANDER KOELPIN** (Senior Member, IEEE) received the Diploma degree in electrical engineering in 2005, the Doctoral degree in 2010, and the "*venia legendi*" in 2014 all from Friedrich-Alexander-University Erlangen-Nuremberg (FAU), Erlangen, Germany. From 2005 to May 2017, he was with the Institute for Electronics Engineering, FAU, Germany. From 2007 to 2010, he was a team leader, from 2010 to 2015, a group leader for Circuits, Systems and Hardware Test, and since 2015, a leader of the group Electronic Systems. From June 2017 to February 2020, he was a Professor and Head of the Chair for Electronics and Sensor Systems with the Brandenburg University of Technology Cottbus-Senftenberg, Germany. Since March 2020, he has been with Hamburg University of Technology, Germany, as a Full Professor and Head of the Institute of High-frequency Technology. He has authored or coauthored more than 300 publications in his areas of interest. His research interests include the areas of microwave circuits and systems, radar and wireless sensing, wireless communication systems, local positioning, and six-port technology. Furthermore, he was a reviewer for several journals and conferences, Chair of the IEEE MTT-S technical committee MTT-16, since 2018 Elected Member, and since 2020 Vice Chair of the IEEE MTT-S/AP German Chapter Executive Board, member of the Commission A: Electromagnetic Metrology of U.R.S.I., and from 2012 to 2017, conference Co-Chair of the IEEE Topical Conference on Wireless Sensors and Sensor Networks. In 2016, he was awarded the IEEE MTT-S Outstanding Young Engineer Award and in 2017, the ITG Award of the German VDE.